Development 134, 2359-2368 (2007) doi:10.1242/dev.001677

BMP signals control limb bud interdigital programmed cell death by regulating FGF signaling

Sangeeta Pajni-Underwood[1], Catherine P. Wilson[1], Cindy Elder[2], Yuji Mishina[3] and Mark Lewandoski[1,*]

In vertebrate limbs that lack webbing, the embryonic interdigit region is removed by programmed cell death (PCD). Established models suggest that bone morphogenetic proteins (BMPs) directly trigger such PCD, although no direct genetic evidence exists for this. Alternatively, BMPs might indirectly affect PCD by regulating fibroblast growth factors (FGFs), which act as cell survival factors. Here, we inactivated the mouse BMP receptor gene *Bmpr1a* specifically in the limb bud apical ectodermal ridge (AER), a source of FGF activity. Early inactivation completely prevents AER formation. However, inactivation after limb bud initiation causes an upregulation of two AER-FGFs, *Fgf4* and *Fgf8*, and a loss of interdigital PCD leading to webbed limbs. To determine whether excess FGF signaling inhibits interdigit PCD in these *Bmpr1a* mutant limbs, we performed double and triple AER-specific inactivations of *Bmpr1a*, *Fgf4* and *Fgf8*. Webbing persists in AER-specific inactivations of *Bmpr1a* and *Fgf8* owing to elevated *Fgf4* expression. Inactivation of *Bmpr1a*, *Fgf8* and one copy of *Fgf4* eliminates webbing. We conclude that during normal embryogenesis, BMP signaling to the AER indirectly regulates interdigit PCD by regulating AER-FGFs, which act as survival factors for the interdigit mesenchyme.

KEY WORDS: Apoptosis, BMP, FGF, Interdigit, Limb development, Programmed cell death

INTRODUCTION

It is becoming increasingly clear that cellular activities such as cell proliferation, apoptosis and migration that contribute to the generation of pattern during development are often regulated by coordinated interactions between two or more signaling cascades. The developing limb provides an excellent model system for studying these interactions, owing to the availability of a rich context of genetic and embryological data (Capdevila and Izpisua Belmonte, 2001; Niswander, 2002; Tickle, 2006).

Vertebrate limbs begin as buds of the lateral plate mesoderm, jacketed in surface ectoderm. In the mouse, at about embryonic day (E) 10.5 and 11.0 in the forelimb and hindlimb bud, respectively, cells have finished moving from the ventral ectoderm of the early bud (the 'preAER') to the bud apex to form a stratified columnar epithelial structure called the apical ectodermal ridge (AER) (Kimmel et al., 2000; Loomis et al., 1998; Guo et al., 2003). Although the AER itself is fated to undergo cell death, it is a source of secreted factors required for limb bud outgrowth. This is demonstrated by the surgical removal of the AER in chick embryos, which results in proximal-distal truncations (Dudley et al., 2002; Saunders, 1948; Summerbell, 1974).

The AER-specific activity required for limb bud outgrowth is encoded by members of the FGF family (reviewed by Martin, 1998). FGF protein can rescue limb development in chick embryos that have a surgically removed AER (Fallon et al., 1994; Niswander et al., 1993). Four Fgf genes (*Fgf4*, *8*, *9* and *17*, referred to here collectively as AER-FGFs) are expressed in the AER (Martin, 1998; Sun et al., 2000). The *Fgf8* expression domain is the largest spatially, being strongly expressed throughout the anterior-posterior extent of the AER, and is also the longest temporally, occurring earliest, in the preAER (Lewandoski et al., 2000), and ending during AER regression (E12.5-13.5) (Crossley et al., 1996; Mahmood et al., 1995; Salas-Vidal et al., 2001). By contrast, the other three AER-FGF genes display more restricted expression domains within the posterior two-thirds of the AER, with expression initiating later and ceasing earlier than *Fgf8* (Sun et al., 2000). In the mouse, single-gene inactivation studies reveal that, of the four AER-FGFs, only *Fgf8* is required for normal limb development, although most limb skeletal elements still form in limb buds lacking *Fgf8* (Colvin et al., 2001; Lewandoski et al., 2000; Moon et al., 2000; Moon and Capecchi, 2000; Sun et al., 2000; Xu et al., 2000). However, when *Fgf4* and *8* are simultaneously inactivated throughout the preAER, mice are born without limbs, indicating that these two Fgf genes are genetically redundant (Sun et al., 2002; Boulet et al., 2004). Thus, *Fgf4* and *8* may be considered the principal AER-FGFs.

Another set of molecules playing a role in limb development are the members of the bone morphogenetic protein (BMP) family, which, in contrast to FGFs, have been implicated in a variety of diverse aspects of limb development including digit identity, anterior-posterior and dorsal-ventral patterning of the limb and AER regulation (Niswander, 2002; Tickle, 2006). Early in limb bud development, BMP signaling is required for normal formation of the AER (Ahn et al., 2001; Pizette et al., 2001). As the AER develops, regulation of BMP activity by the antagonist gremlin is required to activate *Fgf4*, *9* and *17* (Capdevila et al., 1999; Khokha et al., 2003; Michos et al., 2004; Zuniga et al., 1999; Zuniga et al., 2004).

Later in limb development, BMPs also play a role in programmed cell death (PCD) of the interdigit region, which is required to separate digits and prevent soft tissue syndactyly (webbing) (reviewed by Chen and Zhao, 1998; Zuzarte-Luis and Hurle, 2002; Zuzarte-Luis and Hurle, 2005). Prior to cell death, *Bmp2*, *4* and *7* are upregulated within the interdigit mesenchyme (Chen and Zhao, 1998; Hogan, 1996) and inhibition of BMP signaling in chick embryos, via the retroviral expression of transgenes encoding dominant-negative BMP receptors, inhibits interdigit PCD (Yokouchi et al., 1996; Zou and Niswander, 1996). Furthermore, in

[1]Laboratory of Cancer and Developmental Biology and [2]SAIC, NCI-Frederick, National Institutes of Health, Frederick, MD 21702, USA. [3]Laboratory of Reproductive and Developmental Toxicology, National Institute of Environmental Health Sciences, Research Triangle Park, NC, USA.

*Author for correspondence (e-mail: mlewandoski@mail.ncifcrf.gov)

Accepted 10 April 2007

the mouse, syndactylous limbs are caused by inhibiting BMP signaling through the ectopic expression of the BMP antagonist noggin (Guha et al., 2002; Wang et al., 2004).

These data are generally construed to signify that BMPs act as direct effectors of PCD within the interdigit region (Chen and Zhao, 1998; Zou and Niswander, 1996; Zuzarte-Luis and Hurle, 2002; Zuzarte-Luis and Hurle, 2005). However, FGF-soaked beads can prevent interdigital PCD in chick embryos (Buckland et al., 1998; Ganan et al., 1996; Macias et al., 1996; Ngo-Muller and Muneoka, 2000), suggesting that interdigital PCD might be induced by the loss of AER-FGF signaling that occurs during AER regression (Salas-Vidal et al., 2001; Yokouchi et al., 1996; Zou and Niswander, 1996). On the other hand, application of FGF-soaked beads can also increase interdigital apoptosis, consistent with a model of cooperation between FGFs and BMPs acting as cell death triggers (Ganan et al., 1998; Montero et al., 2001). Thus, the relationship between BMP and FGF signaling during interdigital PCD is unclear.

Here, we define a relationship between BMP and FGF signaling during interdigital PCD. First, we inactivate the gene encoding the BMP receptor, *Bmpr1a*, specifically in the limb bud preAER or AER via Cre-mediated DNA recombination. Our data reveal a dynamic role for BMPR1A signaling: early BMP activity is required for AER formation and later activity is required for cessation of AER-FGF expression, which is correlated with interdigital PCD. Then, by analyzing mice carrying different combinations of double and triple AER-specific gene inactivations of *Fgf4*, *8* and *Bmpr1a*, we provide genetic evidence that BMPs regulate interdigit cell death through the regulation of AER-FGF signals.

MATERIALS AND METHODS

Production of mutant embryos

All mutant alleles, the Msx2-Cre transgene and PCR conditions for genotyping these markers have been described previously (Lewandoski et al., 2000; Mishina et al., 2002; Mishina et al., 1995; Sun et al., 2000). Mutants were generated on a mixed CD1/129SvEv/C57BL/6 background. Msx2-Cre*;* $Bmpr1a^{flox/null}$ mice were produced as described in Fig. 1. Msx2-Cre*;* $Bmpr1a^{flox/null}$ mutants that also carry mutated *Fgf4* (or *Fgf8*) alleles were generated by mating $BmpR1a^{flox/flox}$*;* $Fgf4^{flox/flox}$ (or $BmpR1a^{flox/flox}$*;* $Fgf8^{flox/flox}$) females with Msx2-Cre*;* $BmpR1a^{null/wt}$*;* $Fgf4^{null/wt}$ (or with Msx2-Cre*;* $Fgf8^{null/wt}$) males. Likewise, to generate triple mutants, $BmpR1a^{flox/flox}$*;* $Fgf4^{flox/flox}$*,* $Fgf8^{flox/flox}$ females were mated with Msx2-Cre*;* $BmpR1a^{null/wt}$*;* $Fgf4^{null/wt}$*,* $Fgf8^{null/wt}$) males. Noon of the day on which the vaginal plug was detected was considered E0.5. More precise age of E9.5-10.5 embryos was determined by counting the somites posterior to the forelimb, scoring the first as somite 13.

Whole-mount in situ hybridization, β-galactosidase (β-gal) and Lysotracker staining

RNA localization by whole-mount in situ hybridization was performed as described (Pizard, 2004), with a minor change: detection of AER transcripts required no proteinase K treatment. β-gal and Lysotracker Red (Molecular Probes) staining was performed as previously described (Chi et al., 2003; Zucker et al., 1999).

RESULTS

Msx2-Cre inactivation of *Bmpr1a* causes disparate hindlimb and forelimb phenotypes

To study the role of BMP signaling in the limb bud AER, we sought to produce Msx2-Cre*;* $Bmpr1a^{flox/null}$ (or 'mutant') mice so that Msx2-Cre activity in the preAER (Sun et al., 2000) will inactivate the $Bmpr1a^{flox}$ allele. In the course of performing the required genetic crosses, we discovered that the Msx2-Cre transgene is integrated on chromosome 14, very closely linked to the *Bmpr1a* locus. Therefore, in order to generate mutant mice, we needed to first produce mice carrying both the Msx2-Cre transgene and the $Bmpr1a^{null}$ allele in cis on chromosome 14. To achieve this, we screened approximately 1300 progeny of Msx2-Cre*;* $Bmpr1a^{null/+}$ mice crossed to wild-type mice before identifying one offspring with a recombinant chromosome 14 containing both genetic markers. This mouse and its progeny served as sires in the genetic cross indicated in Fig. 1A, in which 50% of the offspring are mutant and 50% ($Bmpr1a^{flox/+}$) are controls.

We and others (Barrow et al., 2003; Sun et al., 2000) have previously shown that Msx2-Cre is active earlier in the prospective AER cells of the hindlimb region where expression is widespread by the 24-somite stage (ss), as compared with the forelimb where extensive expression occurs by 28ss. To determine whether the kinetics of *Bmpr1a* inactivation followed this pattern, we performed RNA in situ hybridization (ISH) on mutant embryos using a riboprobe derived from those sequences in the $Bmpr1a^{flox}$ allele deleted by Cre. Although we could detect *Bmpr1a* expression at E10.5 in the control forelimb (including the AER) and demonstrate *Bmpr1a* inactivation in the mutant AER (Fig. 1A, inset), we could not reproducibly detect *Bmpr1a* expression at limb bud stages prior to AER formation. However, using a full-length *Bmpr1a* riboprobe, we were able to detect expression in the preAER (data not shown), although this riboprobe cannot discriminate between mRNA transcribed from the unrecombined floxed allele and the recombined derivative. Therefore, we conclude that *Bmpr1a* is expressed in the limb bud surface ectoderm/preAER, but below detectable levels when using the floxed *Bmpr1a* sequences as an ISH riboprobe, and we confirm a previous report that these sequences function inadequately as a riboprobe in ISH analysis (Liu et al., 2005).

As an alternative measure of whether the kinetics of Msx2-Cre activity occurred as expected, we stained for the Cre-dependent β-gal activity of the *R26R* reporter allele (Soriano, 1999) in Msx2-Cre*;* $Bmpr1a^{flox/null}$*;* $Rosa26^{R26R/+}$ embryos. As expected, ectoderm in the mutant hindlimb territory was extensively recombined by 24ss, whereas the mutant forelimb preAER was extensively recombined by 28ss (Fig. 1B,C).

Because Msx2-Cre is active earlier in the prospective hindlimb ectoderm relative to forelimb Cre activity, we expected a more severe hindlimb mutant phenotype. We found that in all skeletal preparations examined, mutant hindlimbs never formed (n=16) and the pelvic bones were reduced to two rudimentary elements, each resembling a fused ischium and ilium (Fig. 1D-G). All forelimb skeletal elements were present (n=15), with excess material in the digit tips (n=15) (Fig. 1D,E,H,I). Furthermore, 20% (3 of 15) contained a forelimb preaxial extra digit and 33% (5 of 15) displayed a split preaxial digit (data not shown). Surprisingly, these mutant phenotypes are not similar defects that vary in severity, but rather the hindlimb phenotype (no outgrowth) and the forelimb phenotype (extra outgrowth) are opposite in nature, suggesting that BMP signaling plays a dynamic role during limb development.

No hindlimb PreAER forms in Msx2-Cre*;* $Bmpr1a^{flox/null}$ embryos

The AER is derived from the preAER, a broad domain of thickened ventral limb bud ectoderm (Kimmel et al., 2000). To determine whether the lack of hindlimbs in mutants is due to a failure in preAER/AER formation, we examined histological sections of mutant and control hindlimb buds from E9.5 (31ss) through to E10.5. The morphological preAER and AER were both absent in all mutant hindlimb buds (Fig. 2A-D). We used ISH to assay for expression of *Fgf8*, the earliest expressed AER-FGF, normally present in the hindlimb preAER by 27ss (Lewandoski et al., 2000). At this stage,

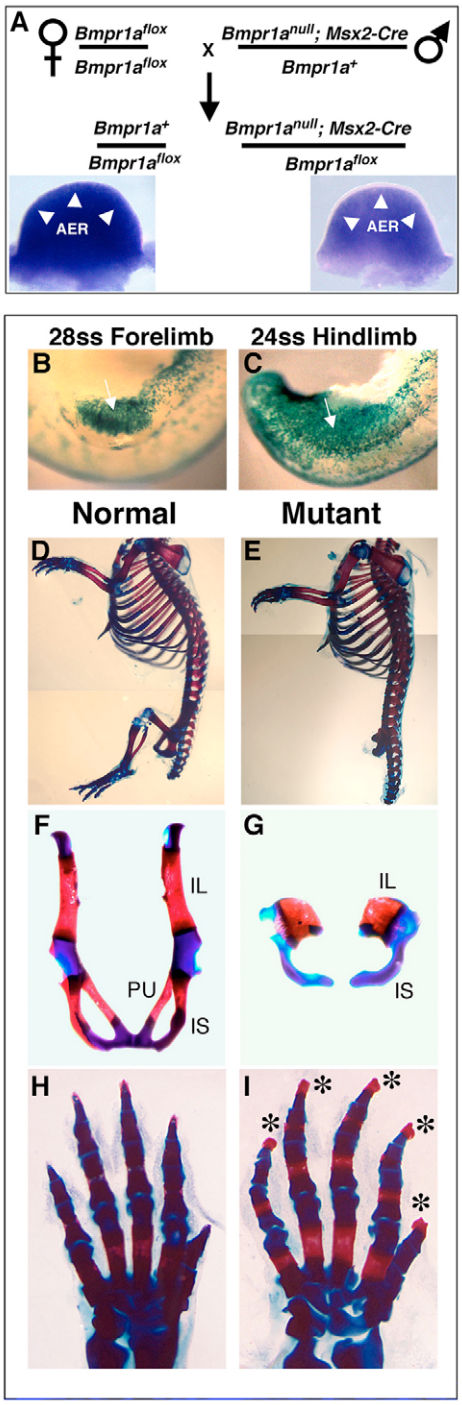

Fig. 1. Skeletal abnormalities in Msx2-Cre*; Bmpr1a*$^{flox/null}$ limbs. (**A**) Mating scheme used to produce mutant (Msx2-Cre*; Bmpr1a*$^{flox/null}$) and control (*Bmpr1a*$^{flox/wt}$) mouse embryos. Inset, dorsal view of E10.5 normal (left) and mutant (right) forelimb buds stained via whole-mount ISH with a riboprobe specific for the Cre-deleted *Bmpr1a* exon. Note the lack of staining (arrowheads) in the mutant AER. (**B**,**C**) Lateral views of early mutant forelimb (B) and hindlimb (C) bud transgenic for the Cre reporter *R26R* and stained for β-gal. Recombination (blue) in limb bud pre-AER (arrows) is extensive at the stages indicated. (**D-I**) Skeletal preparations of normal (D,F,H) and mutant (E,G,I) neonates. In mutants, the hindlimbs are absent (E) and the pelvic bones are reduced or absent (G). Mutant forelimbs contain all skeletal elements (E,I) with broader tips in distal phalanges (asterisks in I). AER, apical ectodermal ridge; IL, ilium; IS, ischium; PU, pubis; ss, somite stage.

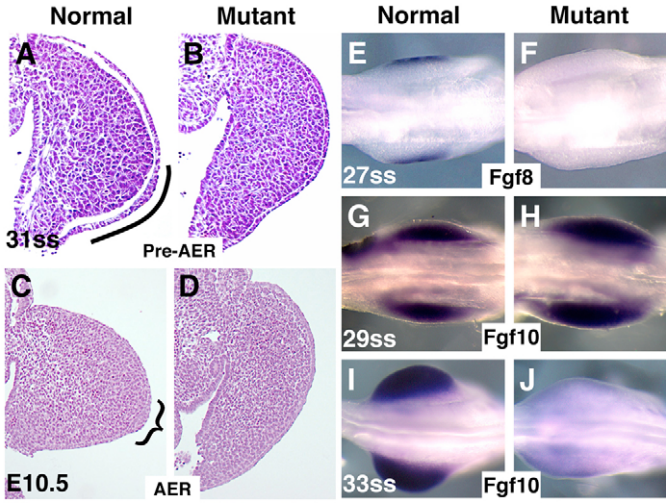

Fig. 2. Lack of a Pre-AER/AER leads to loss of *Fgf10* maintenance in mutant mouse hindimbs. Transverse sections through (**A**,**B**) E9.5 (31ss) and (**C**,**D**) E10.5 hindlimb buds. Note the lack of pre-AER (B) and AER (D) in mutants as compared with normal controls (A,C). (**E-J**) Dorsal views of whole-mount hindlimb bud region stained with the probe at the somite stage indicated. Mutant *Fgf8* expression is not induced (F). Mutant *Fgf10* expression is induced (H) but is not maintained (J).

Fgf8 expression was not detected in mutant hindlimb bud preAER (Fig. 2E,F). Furthermore, we never detected expression of *Fgf8* (or other AER markers: *Fgf4*, *Msx2*, *Jag2*, *Bmp2*, *4* and *7*) at later stages of hindlimb development through to E12.5 (data not shown).

Signals from the AER are required to maintain *Fgf10* expression in the limb bud mesenchyme. Mice lacking *Fgf10* expression do not form limbs (Min et al., 1998; Sekine et al., 1999). *Fgf10* expression was normally induced in mutant hindlimb buds at 29ss (Fig. 2G,H), but maintenance was lost by 33ss (Fig. 2I,J). Thus, we conclude that early *Bmpr1a* inactivation in the hindlimb prevents both the induction of *Fgf8* in the preAER and the formation of a morphological AER. Owing to the lack of AER-FGFs, mesenchymal *Fgf10* expression is not maintained.

Decreased interdigital cell death leads to webbing in Msx2-Cre*; Bmpr1a*$^{flox/null}$ forelimbs

The adult forelimbs of Msx2-Cre*; Bmpr1a*$^{flox/null}$ mice display soft tissue syndactyly (webbing between the digits) (Fig. 7A,B). In the mouse, between E12.5 and E13.5, PCD eliminates cells in the interdigit region, leading to the separation of individual digits (Fernandez-Teran et al., 2006; Zuzarte-Luis and Hurle, 2002; Zuzarte-Luis and Hurle, 2005). To determine whether mutant webbing was due to a PCD defect, we examined E12.5-13.0 control and mutant embryos by staining with the fluorophore Lysotracker Red, and observed a significant reduction in the degree of interdigital cell death in mutant forelimbs (Fig. 3A,B).

Webbing in Msx2-Cre*; Bmpr1a*$^{flox/null}$ forelimbs is not correlated with changes in mesenchymal BMP signaling

BMP signals to the interdigit region have been implicated as direct effectors or triggers of PCD (Ganan et al., 1996; Macias et al., 1997; Merino et al., 1999a; Yokouchi et al., 1996; Zou and Niswander, 1996). Therefore, we examined the expression of genes related to mesenchymal BMP signaling to determine whether mutant forelimb webbing might be explained by *Bmpr1a* inactivation in the AER

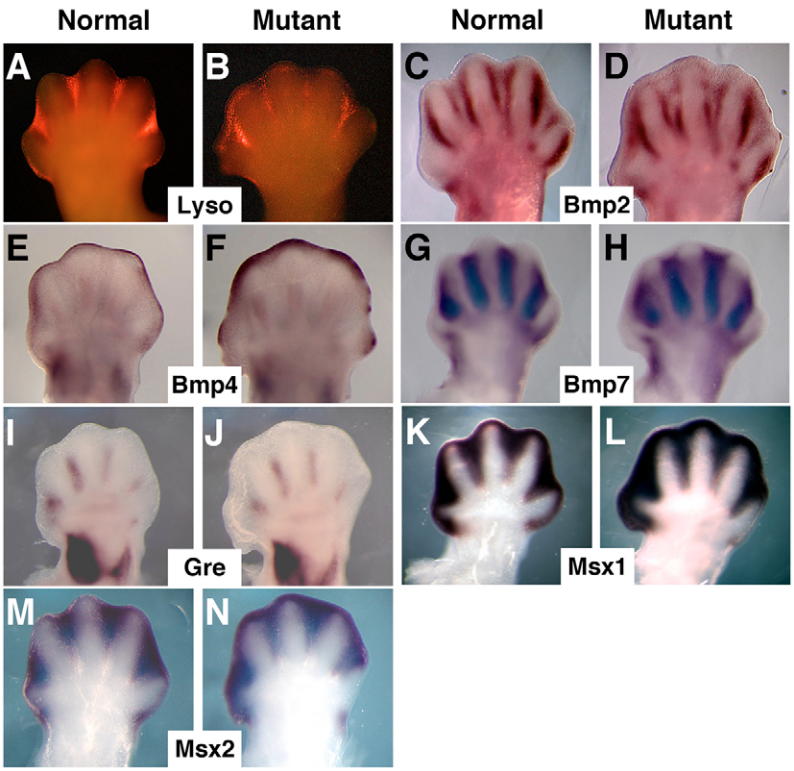

Fig. 3. Reduced interdigital PCD in mutant forelimbs does not correlate with changes in interdigital BMP signaling. (**A**,**B**) Comparison of E13.0 normal (A) and mutant (B) mouse forelimbs stained with the fluorochrome Lysotracker Red to label regions of dying cells. (**C-N**) Whole-mount ISH of E12.5 normal (C,E,G,I,K,M) and mutant (D,F,H,J,L,N) forelimbs for the probes indicated. All are dorsal views, anterior to the left.

indirectly causing a diminution of interdigital BMP signaling. *Bmp2*, *4* and *7* are normally upregulated at E12.5-13.5 in the interdigit region, suggesting that they are candidate ligands for activating BMP signaling in this tissue (Hogan, 1996; Salas-Vidal et al., 2001). All three Bmp genes were induced normally in the interdigit region in both control and mutant E12.5 forelimbs (Fig. 3C-H), with enhanced *Bmp4* expression in mutant subapical mesenchyme (Fig. 3F). Gremlin antagonizes mesenchymal BMP activity (Zuniga et al., 1999) and its enhanced expression in the interdigit region of ducks correlates with the decrease in interdigital PCD occurring in these birds, as compared with chickens (Merino et al., 1999b). However, we found no significant difference between mutants and controls in interdigital gremlin expression (Fig. 3I,J).

The closely related homeobox genes, *Msx1* and *Msx2*, are downstream targets of BMP signaling and are expressed in the PCD zones of the developing limbs, including the interdigit regions (Houzelstein et al., 1997). Furthermore, misexpression of *Msx2* induces cell death in the chick limb bud (Ferrari et al., 1998; Merino et al., 1999b) and $Msx1^{-/-}; Msx2^{-/-}$ embryos retain their interdigit mesenchyme (Lallemand et al., 2005). We detected no decrease in the expression of *Msx1* or *2* in mutant forelimbs at E12.5 (which would have been indicative of a reduction of BMP signaling), but did note an expanded expression domain that is likely to occur as a consequence of the retention of interdigit tissue (Fig. 3K-N).

AER-specific *Msx2* expression (Coelho et al., 1991; Ferrari et al., 1998) was however absent in Msx2-Cre*;* $Bmpr1a^{flox/null}$ forelimbs from E10.5-12.5 (Fig. 4A,B and data not shown), demonstrating that *Msx2* is downstream of BMPR1A signaling in the AER. We also detected a reduction of AER-specific expression of *Bambi* (Fig. 4C-F), which is also a BMP target and encodes a natural dominant-negative BMP receptor (Onichtchouk et al., 1999). Together, these data suggest that only AER-specific BMP targets are affected in Msx2-Cre*;* $Bmpr1a^{flox/null}$ forelimbs, and that mesenchymal BMP-signaling is relatively normal.

Fgf4 and *Fgf8* are upregulated in the forelimb AER of Msx2-Cre*;* $Bmpr1a^{flox/null}$ mutants

To analyze AER function in mutant forelimbs, we examined the expression of the four AER-FGFs (*Fgf4*, *8*, *9* and *17*). We found no significant changes in *Fgf9* expression, but did note a slight increase in *Fgf17* expression (data not shown). At 22ss, we detected no

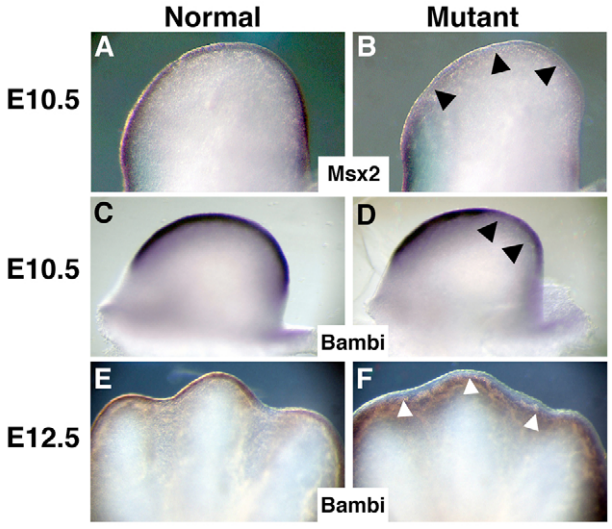

Fig. 4. AER-specific expression of *Msx2* and *Bambi* are downregulated in mutant forelimb. Whole-mount ISH using probes specific for *Msx2* (**A**,**B**) and *Bambi* (**C-F**) in normal (A,C,E) and mutant (B,D,F) mouse forelimb buds at the embryonic stages indicated. At E10.5, mutant *Msx2* expression is absent (arrowheads in B), whereas mutant *Bambi* expression is reduced at E10.5 (arrowheads in D) and absent by E12.5 (arrowheads in F) specifically in the AER, although expression is extended in the subapical mesenchyme (F).

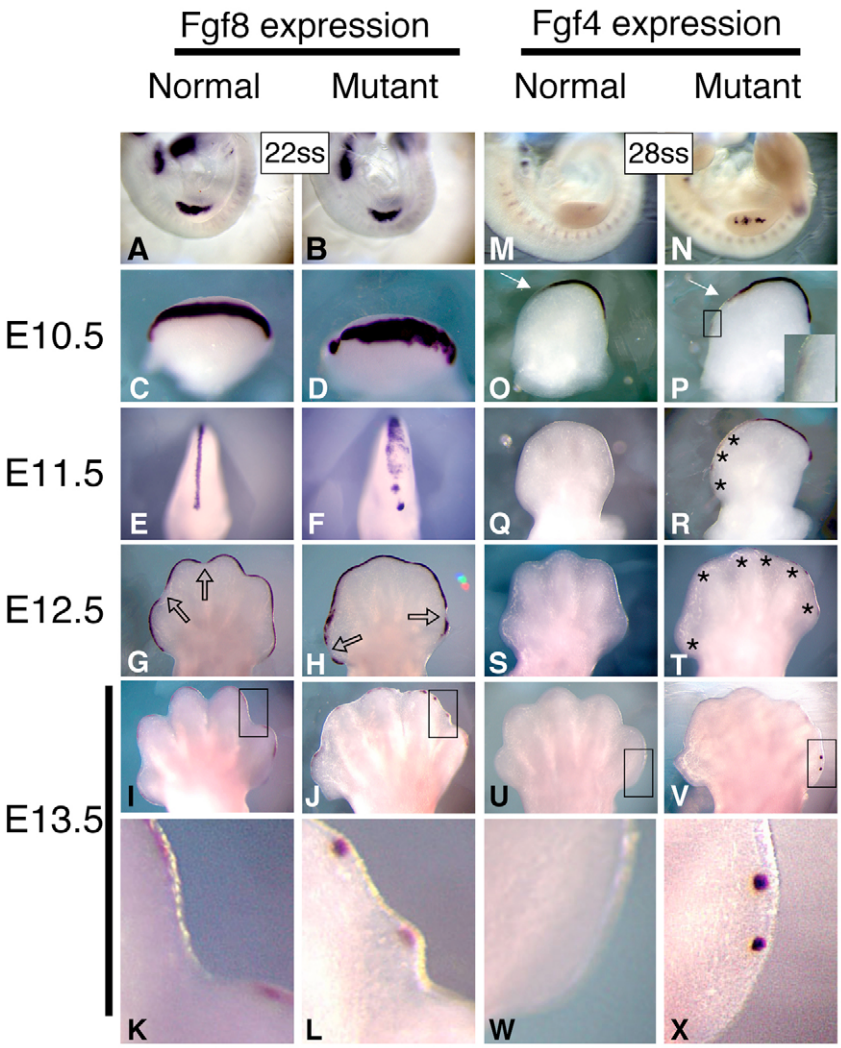

Fig. 5. *Fgf4* and *Fgf8* expression is upregulated in mutant forelimbs. (**A-L**) *Fgf8* and (**M-X**) *Fgf4* expression in normal and mutant mouse forelimbs at the somite or embryonic stage indicated. A,B,M,N are lateral views; C,D are distal views, dorsal toward the top; E,F are anterior views; in all other panels (i.e. G-L,O-X), dorsal views are shown with anterior to the left. *, aberrant expression. The boxed region in P is shown at high magnification in the inset; boxes in I,J,U,V indicate the regions shown at high magnification in K,L,W,X, respectively. The arrow in G indicates lack of *Fgf8* expression over the interdigital region in normal forelimbs; the arrow in H indicates discontinuous *Fgf8* expression in the AER in mutant forelimbs.

change in *Fgf8* expression between normal and mutant forelimbs (Fig. 5A,B). However, by E10.5 (approximately 24 hours after forelimb Msx2-Cre activation), *Fgf8* expression in the mutant forelimb was less constricted dorsal-ventrally, but normally extended anterior-posteriorly (Fig. 5C,D). At E11.5, this expanded *Fgf8* pattern was more pronounced in the anterior AER of mutant forelimbs (Fig. 5E,F) relative to the posterior AER. By E12.5, normal AER-specific *Fgf8* expression was ceasing over the interdigit region, but remained over the developing digits (Fig. 5G), consistent with published reports (Crossley and Martin, 1995; Salas-Vidal et al., 2001). However, in Msx2-Cre*; Bmpr1a* mutants, this cessation of *Fgf8* expression failed to occur, although we did note some infrequent small discontinuities in *Fgf8* expression at the anterior and posterior end of the AER that did not correlate with the digit/interdigit pattern (Fig. 5H). By E13.5, normal *Fgf8* expression was present only over the digits (Fig. 5I,K), whereas punctate *Fgf8* expression occurred throughout the mutant AER (Fig. 5J,L), with regions of expression still present in the interdigit region associated with convex outgrowths of the distal autopod (see Fig. 5K,L). Normal AER *Fgf8* expression completely ceased by E14.5, although mutant expression could still be detected at E15.5 (data not shown).

As with *Fgf8* expression, mutant AER-specific *Fgf4* expression is upregulated. Normally, *Fgf4* expression is first activated at about 28-29ss in a few cells in the posterior AER, and then by E10.5 is restricted to about two-thirds of the posterior AER (Fig. 5M,O) (Niswander and Martin, 1992; Sun et al., 2000). In mutants, *Fgf4* activation occurred more extensively in the anterior-posterior axis and in several distinct patches (Fig. 5N), and by E10.5 extended more anteriorly with some anterior discontinuities in expression (Fig. 5P). By E11.5, *Fg4* expression had ceased in normal forelimbs, whereas in mutants expression remained robust in the posterior region of the AER with weaker expression in the anterior AER (Fig. 5Q,R). Punctate AER-specific expression of *Fgf4* remained through E12.5 and E13.5 (Fig. 5S-X).

To determine whether the expression of other AER markers was temporally extended, we examined *Bmp2*, *4* and *7* expression in the mutant AER at E12.5-13.5. *Bmp4* expression was not upregulated in the AER, although expression was increased in the subapical region (Fig. 3F and data not shown). At these stages, mutant AER-specific expression of *Bmp2* and *7* was either absent or upregulated in a few posterior cells (*Bmp2*, 3 of 13 limbs; *Bmp7*, 5 of 7 limbs) (data not shown). Thus, considering the extent of their upregulation, *Fgf4* and *8* were uniquely affected, owing to the lack of BMPR1A-mediated signaling to the AER.

FGF4 and FGF8 act as survival factors for the interdigit region

The upregulation of the principal AER-FGFs (*Fgf4* and *8*) in mutant forelimbs raises the possibility that webbing might be due to prolonged expression of these FGFs acting as survival factors for the

underlying interdigital mesenchyme. To test this, we examined webbing in mutant animals in which we genetically lowered the AER-FGF levels in the forelimb AER by generating Msx2-Cre; *Bmpr1a*$^{flox/null}$ animals that also carry null or floxed alleles of *Fgf4* and/or *8*. However, we could not assess the complete contribution of both *Fgf4* and *8* to the mutant webbing phenotype (i.e. in animals of the genotype Msx2-Cre; *Bmpr1a*$^{flox/null}$; *Fg4*$^{flox/null}$; *Fgf8*$^{flox/null}$) because Msx2-Cre inactivation of both Fgf genes causes a severe disruption of limb development, preventing analysis of interdigital PCD (Sun et al., 2002). Nevertheless, we could evaluate the effect of less extreme genotypes (i.e. with at least one copy of *Fgf4* or *Fgf8* intact), which reduce AER FGF4/8 activity to a level above zero, on the webbing phenotype of Msx2-Cre; *Bmpr1a*$^{flox/null}$ progeny.

Webbing was essentially unchanged in mutant mice with Msx2-Cre-mediated deletion of *Fgf4* in the AER (Msx2-Cre; *Bmpr1a*$^{flox/null}$; *Fgf4*$^{flox/null}$) (data not shown). Similarly, mutant mice that lacked *Fgf8* expression in the AER (Msx2-Cre; *Bmpr1a*$^{flox/null}$; *Fgf8*$^{flox/null}$) possessed webbed limbs (Fig. 7B,C). However, we noted that the forelimbs of these animals contained all five digits (n=16 limbs) (Fig. 6C; Fig. 7C), which was surprising because Msx2-Cre-mediated deletion of *Fgf8* (Msx2-Cre; *Fgf8*$^{flox/null}$) causes a hypodactyly phenotype in which at least one and occasionally two digits fail to form (Fig. 6A,B) (Lewandoski et al., 2000). Thus, this hypodactyly phenotype was rescued in Msx2-Cre; *Bmpr1a*$^{flox/null}$; *Fgf8*$^{flox/null}$ animals. We speculated that the levels of *Fgf4* expression in Msx2-Cre; *Bmpr1a*$^{flox/null}$; *Fgf8*$^{flox/null}$ animals might be above a threshold level required to rescue digit formation and maintain lower interdigit PCD. We also reasoned that *Fgf4* expression levels in Msx2-Cre; *Fgf8*$^{flox/null}$ animals, although elevated (Lewandoski et al., 2000), might be below this threshold as hypodactyly but no webbing occurs in these mutants. Indeed, semi-quantitative ISH revealed that *Fgf4* expression in E11.5 and E12.5 forelimbs was higher in Msx2-Cre; *Bmpr1a*$^{flox/null}$; *Fgf8*$^{flox/null}$ than in forelimbs in which only *Fgf8* had been deleted by Msx2-Cre (Fig. 6D-I).

Next we examined the phenotype of mutant animals in which only one copy of *Fgf8* was deleted (i.e. of the genotype *Bmpr1a*$^{flox/null}$; *Fgf8*$^{flox/+}$, or *Bmpr1a*$^{flox/null}$; *Fgf8*$^{null/+}$; n=26 limbs). We reasoned that webbing might be reduced in these mice because we do not expect a compound increase in *Fgf4* expression as *Fgf8* heterozygotes do not affect AER *Fgf4* expression (Lewandoski et al., 2000). Webbing was partially reduced to a variable extent in this genotype (Fig. 7D). Lastly, we found that reducing FGF4 levels by generating Msx2-Cre; *Bmpr1a*$^{flox/null}$; *Fgf4*$^{null/+}$; *Fgf8*$^{flox/null}$ animals resulted in forelimbs in which interdigit PCD was rescued as these limbs displayed little or no webbing (n=14 limbs) (Fig. 7E,F). Furthermore, the hypodactyly phenotype due to loss of *Fgf8* (Lewandoski et al., 2000) was usually restored (10 of 14 forelimbs had four digits and two of 14 had three digits, and in each of six skeletal preparations generated, at least one digit lacked a phalanx, see Fig. 7F inset), demonstrating that elevated AER *Fgf4* expression rescues digit formation and causes webbing in the absence of *Fgf8* and *Bmpr1a*. Taken together, these data provide genetic evidence that normal interdigit PCD is regulated by the BMP-mediated downregulation of AER-FGFs, which act as cell survival factors of the interdigit mesenchyme.

DISCUSSION

By specifically inactivating the BMP receptor *Bmpr1a* in the AER of the limb bud, we uncover three aspects of BMP signaling during limb development. First, we demonstrate that BMPR1A-mediated signals are required early to induce the morphological preAER, and then later to extinguish normal AER-FGF expression; these

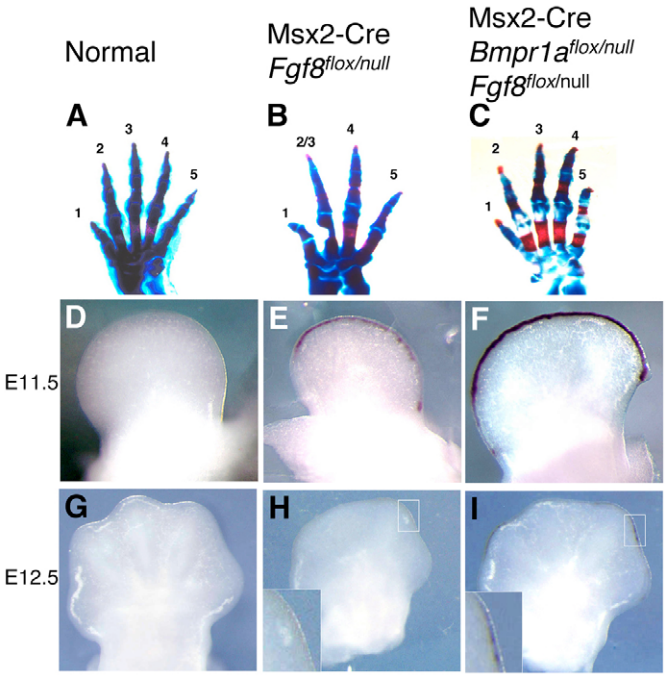

Fig. 6. Inactivation of *Bmpr1a* rescues hypodactyly in Msx2-Cre; *Fgf8*$^{flox/null}$ mouse forelimbs. (**A-C**) Skeletal preparation of forelimbs of the genotypes indicated. Individual digits are numbered. Note that hypodactyly in Msx2-Cre; *Fgf8*$^{flox/null}$ mutants (B) is rescued by also deleting *Bmpr1a* (C). (**D-I**) Dorsal views (anterior to left) of forelimbs of the embryonic age and genotype indicated, stained with an *Fgf4* riboprobe for a short time period (2 hours, 4°C) to optimally visualize differences in *Fgf4* expression levels. *Fgf4* expression ceases in normal forelimbs by E11.5 (D), but continues in Msx2-Cre; *Fgf8*$^{flox/null}$ mutants through E12.5 (E,H). This enhanced expression is higher in Msx2-Cre; *Bmpr1a*$^{flox/null}$; *Fgf8*$^{flox/null}$ mutants (F,I). Note also that Msx2-Cre *Fgf8*$^{flox/null}$ limb buds are smaller (E,H) than normal (D,G), prefiguring the hypodactyly phenotype (Lewandoski et al., 2000). This size difference is rescued in the double mutants (F,I). The boxed regions in H and I are shown at high magnification in the insets.

experiments confirm and extend previous studies (Ahn et al., 2001; Pizette et al., 2001; Soshnikova et al., 2003; Zou and Niswander, 1996). Second, we demonstrate that a secreted signal, downstream of *Bmpr1a*, emanating from the early limb bud ectoderm to the underlying lateral plate mesenchyme, is required for normal pelvic bone development. Lastly, we define a relationship between BMP and FGF signaling and the roles that these pathways play during interdigital PCD. We provide genetic evidence that BMP signaling to the AER is required for the patterned downregulation of Fgf gene expression, which in turn encodes cell survival activity for the interdigit tissue.

BMP signals are required for AER induction and cessation of AER-FGF expression

Msx2-Cre is active before formation of the hindlimb preAER but after forelimb preAER induction (Sun et al., 2000). In other studies, in which Msx2-Cre has been used to study preAER/AER gene function, this pattern resulted in a phenotype that affected the hindlimb more than the forelimb (Barrow et al., 2003; Lewandoski et al., 2000; Pan et al., 2005; Sun et al., 2000; Sun et al., 2002). However, in the case of Msx2-Cre-mediated *Bmpr1a* inactivation, opposite phenotypes are observed: forelimb AER function is longer-

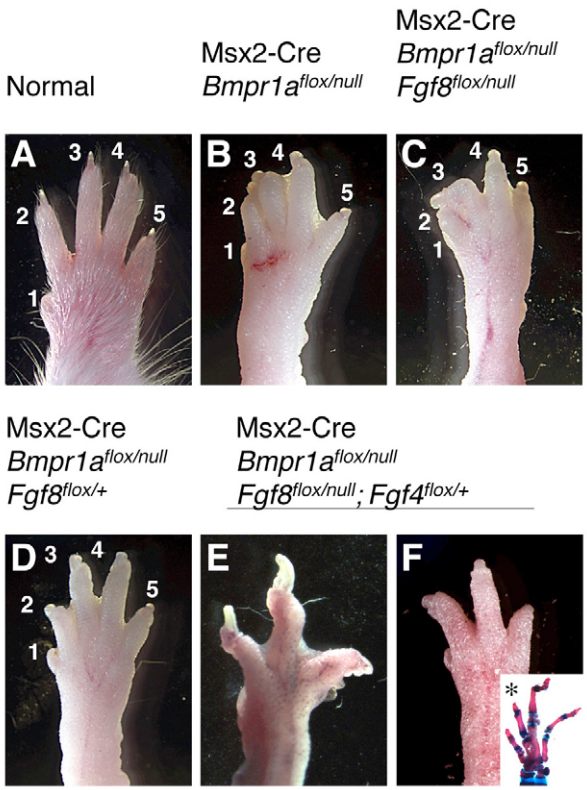

Fig. 7. Reduction of AER-FGF dose rescues syndactyly in Msx2-Cre; *Bmpr1a*$^{flox/null}$ mouse forelimbs. (**A-F**) Dorsal view of forelimbs (anterior to left) of the genotype shown. Interdigital webbing occurs owing to Msx2-Cre-mediated inactivation of *Bmpr1a* (B), even when *Fgf8* is also inactivated (C). However, note that loss of *Bmpr1a* rescues the hypodactyly phenotype due to Msx2-Cre-mediated inactivation of *Fgf8* (C) (also see Fig. 6). (D) Inactivation of one copy of *Fgf8* partially rescues webbing in Msx2-Cre; *Bmpr1A*$^{flox/null}$ forelimbs. (E,F) Inactivation of one copy of *Fgf4* mostly rescues webbing in Msx2-Cre; *Bmpr1A*$^{flox/null}$; *Fgf8*$^{flox/null}$ forelimbs, as well as restoring the hypodactyly phenotype resulting from loss of *Fgf8*. The inset in F is a skeletal preparation showing hypodactyly and a missing phalange (*). All animals were approximately 8 weeks of age, except for that in E which was 3 months of age, which accounts for the longer nails of this limb. Note that owing to Msx2-Cre expression in the hair follicle (Pan et al., 2004), Msx2-Cre; *Bmpr1a*$^{flox/null}$ animals (B-F) have a hair phenotype.

lived owing to prolonged AER-FGF expression, whereas the hindlimb preAER/AER never forms. We have performed confocal imaging of forelimb interdigit mutant and normal ectoderm at E12.5-E13.5 and could not demonstrate a longer-lived morphological AER (data not shown). Moreover, we examined cell proliferation (by immunostaining for phosphorylated histone H3) and cell death (by Lysotracker Red staining) in the normal and mutant forelimb AER, and found no qualitative differences between the two (data not shown). Therefore, we do not suggest that BMPR1A signaling is required for the normal regression of the AER that occurs at about E12.5, but rather that BMPR1A signals specifically regulate the cessation of AER-FGF expression.

It is formally possible that the different Msx2-Cre; *Bmpr1a*$^{flox/null}$ AER phenotypes reflect inherent differences in BMP signaling between forelimb and hindlimb development. However, we reject this idea on the basis of work undertaken in chick embryos, in which the results of manipulations of BMP signaling in both wing and leg bud development at early and late embryological time points are more consistent with a dynamic role for BMP signaling within each limb bud (Pizette et al., 2001; Pizette and Niswander, 1999). Thus, we interpret our data as supporting a hypothesis in which, within each limb bud, BMP signals to the early ectoderm are required to induce the preAER, and later signals to the AER are required to cease AER-FGF expression. This is consistent with the data of Ahn et al. (Ahn et al., 2001), in which a variable degree of hindlimb AER disruption occurred due to the AER-specific inactivation of *Bmpr1a*. The Cre line used by Ahn et al. is active in the hindlimb ectoderm at about E9.75, which is later than Msx2-Cre activation (at 24ss, ~E9.5). Hence we propose that E9.75 is in the temporal window when BMP signaling is beginning to cease functioning in hindlimb AER induction.

The molecular basis for this switch in BMP function might be an intrinsic property of preAER/AER cells, i.e. over time the competence of these cells changes such that at early stages they respond to BMPR1A signals by forming an AER, and at later stages by shutting down AER-FGF expression. Alternatively, the integration of BMP with other signals might translate to different cellular behaviors. In support of this, mesenchymal FGF10 signals and ectodermal WNT3 signals are both required for AER formation (Barrow et al., 2003; Min et al., 1998; Sekine et al., 1999).

A preAER signal is required for normal hip girdle formation

Surgical removal of chick ectoderm prior to limb bud formation prevents normal pelvic bone development, suggesting that a preAER factor signals to the lateral flank mesoderm for pelvic girdle development (Malashichev et al., 2005). Also, certain mouse mutations that prevent hindlimb AER induction also affect pelvic bone development, including defects in *p63* (*Trp63* – Mouse Genome Informatics), *Wnt3* or *β-catenin* (Barrow et al., 2003; Mills et al., 1999; Yang et al., 1999). Our observation that the pelvic bones in Msx2-Cre; *Bmpr1a*$^{flox/null}$ mice are reduced to two elements resembling rudimentary ischia/ilia, indicates that the preAER factor is downstream from BMPR1A and secreted from the Msx2-Cre expression domain.

Pelvic bones are also diminished in *Fgf10*$^{-/-}$ animals (Min et al., 1998; Sekine et al., 1999). Given that mesenchymal *Fgf10* expression is not maintained in Msx2-Cre; *Bmpr1a*$^{flox/null}$ hindlimb buds (owing to a lack of AER-FGF signals), one might consider that loss of *Fgf10* expression causes the Msx2-Cre; *Bmpr1a*$^{flox/null}$ pelvic girdle phenotype. However, we speculate that this is not the case, because *Fgf10* expression is also not maintained in Msx2-Cre; *Fgf4*$^{flox/null}$; *Fgf8*$^{flox/null}$ mice and yet there is no similar pelvic bone phenotype in these mutants (Sun et al., 2002). [A very subtle pelvic bone phenotype occurs, but with all pelvic bones present in Msx2-Cre; *Fgf4*$^{flox/null}$; *Fgf8*$^{flox/null}$ mutants (B. Rosenman and C. O. Lovejoy, personal communication)]. Indeed, our observations suggest the novel interpretation that the *Fgf10*$^{-/-}$ pelvic girdle phenotype might be non-cell-autonomous in that it could be a secondary effect resulting from the lack of a preAER signal.

Consideration of the relatively normal pelvic bones in Msx2-Cre; *Fg4*$^{flox/null}$; *Fgf8*$^{flox/null}$ mutants also indicates that neither of the principal AER-FGFs, FGF4 and FGF8, is the secreted factor downstream of BMPR1A required for pelvic development. WNT signaling might be involved as BMPR1A has been shown to control WNT-mediated limb bud outgrowth (Soshnikova et al., 2003) and Msx2-Cre inactivation of *Wnt3* similarly affects pelvic bone development (Barrow et al., 2003).

BMP signals control interdigital PCD by regulating AER-FGF expression

In Msx2-Cre; *Bmpr1a*$^{flox/null}$ mutants, a lack of normal interdigital PCD causes forelimb cutaneous syndactyly to occur between all forelimb digits. During normal development, elevated BMP levels within the interdigit region have been proposed to be a direct effector of cell death within this region (Zuzarte-Luis and Hurle, 2002; Zuzarte-Luis and Hurle, 2005). However, no change indicative of a reduction of BMP signaling occurred in the mesenchymal gene expression levels of BMP ligands (*Bmp2*, *4* and *7*), the antagonist gremlin, or the downstream targets *Msx1* and *2*, indicating that this proposed BMP role does not cause mutant webbing. Instead, a prolonged period of AER *Fgf4* and *Fgf8* expression occurred in mutants. By examining Msx2-Cre; *Bmpr1a*$^{flox/null}$ mutants in which we reduced AER-FGF activity by also inactivating *Fgf4* and/or *8*, we observed a partial rescue of normal interdigit PCD with one copy of *Fgf8* inactivated, and a more complete rescue with both copies of *Fgf8* and one copy of *Fgf4* inactivated. Thus, we provide genetic evidence that one mechanism by which BMPs can regulate interdigit PCD is through the regulation of AER-FGFs acting as cell survival factors.

In the course of these experiments, we found that inactivation of both copies of *Fgf8* (with both *Fgf4* copies intact) in Msx2-Cre; *Bmpr1a*$^{flox/null}$ mutants did not rescue normal interdigit development because such rescue was prevented by elevated *Fgf4* expression levels that were higher than the elevation due to loss of *Fgf8* alone. This elevated *Fgf4* expression rescued the hypodactyly that occurs in Msx2-Cre; *Fgf8*$^{flox/null}$ mutants, and hypodactyly was restored when FGF4 levels were reduced (in Msx2-Cre; *Bmpr1a*$^{flox/null}$; *Fgf8*$^{flox/null}$; *Fgf4*$^{flox/+}$ mutants). These data demonstrate that FGF4 can replace FGF8 function in both normal digit development and abnormal repression of interdigit cell death. Consistent with this, Msx2-Cre-mediated ectopic expression of *Fgf4* has been shown to rescue limb development in Msx2-Cre; *Fgf8*$^{flox/null}$ mutants as well as cause cutaneous syndactyly (Lu et al., 2006). However, given that during normal development, AER *Fgf4* expression ceases by E11.5 (Lewandoski et al., 2000) and that *Fgf8* expression ceases at E12.5 first over the interdigit regions preceding interdigital cell death (Salas-Vidal et al., 2001), we postulate that FGF8, not FGF4, is the principal AER-FGF that maintains interdigit cell survival, until it is downregulated through BMPR1A-mediated signaling (Fig. 8).

The insight that FGF8 controls interdigital cell death is reminiscent of studies in which *Fgf8* inactivation causes an abnormal increase in cell death in the first branchial arch (Trumpp et al., 1999), the brain (Chi et al., 2003; Storm et al., 2003), the early limb bud (Moon and Capecchi, 2000; Sun et al., 2002) and the kidney (Grieshammer et al., 2005; Perantoni et al., 2005). However, the current study is the first report demonstrating that the embryo regulates *Fgf8* expression to control normal cell death during development.

Our genetic experiments support speculations, based on gene expression patterns (Salas-Vidal et al., 2001) and the effects of FGF-bearing bead insertion into chick limb buds (Montero et al., 2001; Macias et al., 1996), that AER FGF8 activity might act as a cell survival activity for the interdigit region. Genetic proof for this idea was not obtainable by a simple Msx2-Cre-mediated inactivation of *Fgf8* itself (in which one would expect premature interdigit cell death), because the overall development of the autopod is retarded (Lewandoski et al., 2000). However, this model is supported by the observation that cutaneous syndactyly in the classical human craniosynostosis syndrome, Pfeiffer's, is caused by mutations causing constitutive signaling of the FGFR2c isoform, which is active in limb bud mesenchyme and is thought to act as an FGF8 receptor. Also, we propose that excess AER-FGF activity might be

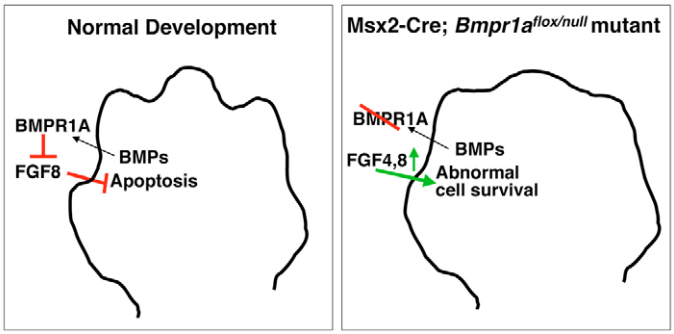

Fig. 8. Model for BMP and FGF interaction during interdigital PCD in normal and mutant mouse limb development. During normal development (left), BMP signaling from the interdigit region signals to the BMPR1A in the AER, causing downregulation of *Fgf8*. FGF8 normally prevents apoptosis in the interdigit region; therefore its downregulation allows interdigit PCD to occur. In Msx2-Cre; *BmpR1A*$^{flox/null}$ forelimb buds (right), BMPR1A is absent, *Fgf4* and *Fgf8* expression persists and abnormal cell survival occurs.

the mechanism by which syndactyly occurs in a number of mouse mutants in which an expanded AER is evident, which include mouse lines carrying mutations affecting the NOTCH and WNT pathways (Jiang et al., 1998; Mukhopadhyay et al., 2001; Pan et al., 2005; Sidow et al., 1997). This proposal can be tested directly by specifically inactivating *Fgf4* and *8* in the AER of these mutants as we have done here.

A supernumerary pre-axial digit occurs in 25% of Msx2-Cre; *Bmpr1a*$^{flox/null}$ forelimbs, as well as in other mouse mutants with enhanced AER-FGF signaling (Adamska et al., 2003; Lu et al., 2006; MacDonald et al., 2004; Wang et al., 2004). However, the prolonged AER-FGF expression in mutant forelimbs was not associated with the formation of extra phalanges. This contrasts with what has been observed in chick embryos, in which prolongation of AER *Fgf8* expression can cause an additional penultimate phalange within a digit, supporting a model in which the duration of AER FGF8 signaling controls elongation of digit primordia and the normal decrease in AER FGF8 signaling generates digit tip formation (Sanz-Ezquerro and Tickle, 2003). The discrepancy between these studies may be explained by inherent differences in AER FGF8 function between mouse and chick limb buds. Alternatively, extra phalange development might also require enhanced SHH as well as FGF8 signaling, considering that AER *Fgf8* expression was prolonged in the chick studies by the insertion of SHH-soaked beads in the underlying mesenchyme (Sanz-Ezquerro and Tickle, 2003). However, consistent with these chick studies we did observe thickened digit tips in all Msx2-Cre; *Bmpr1a*$^{flox/null}$ forelimbs.

In our model (Fig. 8), we propose that FGF8 acts as a cell survival factor for the interdigit region; its normal downregulation via BMPR1A-mediated signals allows interdigit PCD to occur. In our mutant model, *Bmpr1a* inactivation results in prolonged FGF4 and FGF8 signaling, leading to abnormal cell survival and webbed limbs. What is the source of these interdigital BMP signals during normal development? We have examined Bmp gene expression in the AER prior to and during the initiation of interdigital PCD (E12.5-13.5), and found that that *Bmp2* and *7* are not expressed in the AER, whereas *Bmp4* is specifically expressed in the AER/subapical region overlying the digits. However, because *Bmp2*, *4* and *7* are upregulated in the interdigit mesenchyme prior to PCD (Hogan, 1996; Salas-Vidal et al., 2001), we speculate in our model

that this tissue is the BMP source. It is tempting to further speculate that elevated BMP activity during development of the digits, as chondrogenesis proceeds (Yoon and Lyons, 2004), might cause the cessation of AER *Fgf8* expression overlying the digits. Also, earlier studies that described the inhibition of interdigit PCD in chick embryos through the blocking of BMP signaling with retroviral expression of transgenes encoding dominant-negative BMP receptors (Yokouchi et al., 1996; Zou and Niswander, 1996), may be reinterpreted in the context of our model as these retroviral vectors might have inhibited BMP signaling to the AER, elevating Fgf gene expression. Alternatively, our demonstration that BMPs regulate interdigital cell death through the regulation of AER-FGF expression does not exclude a direct role for BMPs as effectors of cell death. Evaluating such a role requires the inactivation of Bmp receptor genes specifically within the interdigit region without affecting AER morphology or gene expression.

Lastly, these data have significant implications for the evolution of limb morphology. Considering the well-established role that the AER plays in the outgrowth of skeletal limb elements, it has been proposed that evolutionary changes in AER-FGF activity might reduce or extend the different cartilaginous and bony limb structures that occur in different species (Cohn and Tickle, 1999; Freitas et al., 2006; Richardson and Oelschlager, 2002; Thewissen et al., 2006). The data presented here suggest that evolutionary alterations in AER-FGF activity might also contribute to the shaping of soft-tissue structure in vertebrates, resulting in normal free digits or webbed limbs. For example, a recent study provides evidence that FGF8-mediated signaling is pivotal in maintaining the interdigit webs in the bat wing (Weatherbee et al., 2006). Future studies into the targets of AER-FGF activity and the interaction of FGF signaling with other pathways are needed to understand how AER-FGF signaling differentially affects the patterning of bony structures and soft tissue.

This research was supported by the Intramural Research Program of the NIH, National Cancer Institute, Center for Cancer Research. We thank L. Grotewold for the *Bambi* probe; J. Matta for expert technical assistance; B. Rosenman and O. Lovejoy for helpful discussion on pelvic bone development; S. Mackem, N. Moore, L. Niswander, A. Perantoni, X. Sun and T. Yamaguchi for manuscript comments; and L. Niswander for making data available prior to publication.

References

Adamska, M., MacDonald, B. T. and Meisler, M. H. (2003). Doubleridge, a mouse mutant with defective compaction of the apical ectodermal ridge and normal dorsal-ventral patterning of the limb. *Dev. Biol.* **255**, 350-362.

Ahn, K., Mishina, Y., Hanks, M. C., Behringer, R. R. and Crenshaw, E. B., 3rd (2001). BMPR-IA signaling is required for the formation of the apical ectodermal ridge and dorsal-ventral patterning of the limb. *Development* **128**, 4449-4461.

Barrow, J. R., Thomas, K. R., Boussadia-Zahui, O., Moore, R., Kemler, R., Capecchi, M. R. and McMahon, A. P. (2003). Ectodermal Wnt3/beta-catenin signaling is required for the establishment and maintenance of the apical ectodermal ridge. *Genes Dev.* **17**, 394-409.

Boulet, A. M., Moon, A. M., Arenkiel, B. R. and Capecchi, M. R. (2004). The roles of Fgf4 and Fgf8 in limb bud initiation and outgrowth. *Dev. Biol.* **273**, 361-372.

Buckland, R. A., Collinson, J. M., Graham, E., Davidson, D. R. and Hill, R. E. (1998). Antagonistic effects of FGF4 on BMP induction of apoptosis and chondrogenesis in the chick limb bud. *Mech. Dev.* **71**, 143-150.

Capdevila, J. and Izpisua Belmonte, J. C. (2001). Patterning mechanisms controlling vertebrate limb development. *Annu. Rev. Cell Dev. Biol.* **17**, 87-132.

Capdevila, J., Tsukui, T., Rodriquez Esteban, C., Zappavigna, V. and Izpisua Belmonte, J. C. (1999). Control of vertebrate limb outgrowth by the proximal factor Meis2 and distal antagonism of BMPs by Gremlin. *Mol. Cell* **4**, 839-849.

Chen, Y. and Zhao, X. (1998). Shaping limbs by apoptosis. *J. Exp. Zool.* **282**, 691-702.

Chi, C. L., Martinez, S., Wurst, W. and Martin, G. R. (2003). The isthmic organizer signal FGF8 is required for cell survival in the prospective midbrain and cerebellum. *Development* **130**, 2633-2644.

Coelho, C. N., Krabbenhoft, K. M., Upholt, W. B., Fallon, J. F. and Kosher, R. A. (1991). Altered expression of the chicken homeobox-containing genes GHox-7 and GHox-8 in the limb buds of limbless mutant chick embryos. *Development* **113**, 1487-1493.

Cohn, M. J. and Tickle, C. (1999). Developmental basis of limblessness and axial patterning in snakes. *Nature* **399**, 474-479.

Colvin, J. S., Green, R. P., Schmahl, J., Capel, B. and Ornitz, D. M. (2001). Male-to-female sex reversal in mice lacking fibroblast growth factor 9. *Cell* **104**, 875-889.

Crossley, P. H. and Martin, G. R. (1995). The mouse Fgf8 gene encodes a family of polypeptides and is expressed in regions that direct outgrowth and patterning in the developing embryo. *Development* **121**, 439-451.

Crossley, P. H., Minowada, G., MacArthur, C. A. and Martin, G. R. (1996). Roles for FGF8 in the induction, initiation, and maintenance of chick limb development. *Cell* **84**, 127-136.

Dudley, A. T., Ros, M. A. and Tabin, C. J. (2002). A re-examination of proximodistal patterning during vertebrate limb development. *Nature* **418**, 539-544.

Fallon, J. F., Lopez, A., Ros, M. A., Savage, M. P., Olwin, B. B. and Simandl, B. K. (1994). FGF-2: apical ectodermal ridge growth signal for chick limb development. *Science* **264**, 104-107.

Fernandez-Teran, M. A., Hinchliffe, J. R. and Ros, M. A. (2006). Birth and death of cells in limb development: a mapping study. *Dev. Dyn.* **235**, 2521-2537.

Ferrari, D., Lichtler, A. C., Pan, Z. Z., Dealy, C. N., Upholt, W. B. and Kosher, R. A. (1998). Ectopic expression of Msx-2 in posterior limb bud mesoderm impairs limb morphogenesis while inducing BMP-4 expression, inhibiting cell proliferation, and promoting apoptosis. *Dev. Biol.* **197**, 12-24.

Freitas, R., Zhang, G. and Cohn, M. J. (2006). Evidence that mechanisms of fin development evolved in the midline of early vertebrates. *Nature* **442**, 1033-1037.

Ganan, Y., Macias, D., Duterque-Coquillaud, M., Ros, M. A. and Hurle, J. M. (1996). Role of TGF beta s and BMPs as signals controlling the position of the digits and the areas of interdigital cell death in the developing chick limb autopod. *Development* **122**, 2349-2357.

Ganan, Y., Macias, D., Basco, R. D., Merino, R. and Hurle, J. M. (1998). Morphological diversity of the avian foot is related with the pattern of msx gene expression in the developing autopod. *Dev. Biol.* **196**, 33-41.

Grieshammer, U., Cebrian, C., Ilagan, R., Meyers, E., Herzlinger, D. and Martin, G. R. (2005). FGF8 is required for cell survival at distinct stages of nephrogenesis and for regulation of gene expression in nascent nephrons. *Development* **132**, 3847-3857.

Guha, U., Gomes, W. A., Kobayashi, T., Pestell, R. G. and Kessler, J. A. (2002). In vivo evidence that BMP signaling is necessary for apoptosis in the mouse limb. *Dev. Biol.* **249**, 108-120.

Guo, Q., Loomis, C. and Joyner, A. L. (2003). Fate map of mouse ventral limb ectoderm and the apical ectodermal ridge. *Dev. Biol.* **264**, 166-178.

Hogan, B. L. (1996). Bone morphogenetic proteins in development. *Curr. Opin. Genet. Dev.* **6**, 432-438.

Houzelstein, D., Cohen, A., Buckingham, M. E. and Robert, B. (1997). Insertional mutation of the mouse Msx1 homeobox gene by an nlacZ reporter gene. *Mech. Dev.* **65**, 123-133.

Jiang, R., Lan, Y., Chapman, H. D., Shawber, C., Norton, C. R., Serreze, D. V., Weinmaster, G. and Gridley, T. (1998). Defects in limb, craniofacial, and thymic development in Jagged2 mutant mice. *Genes Dev.* **12**, 1046-1057.

Khokha, M. K., Hsu, D., Brunet, L. J., Dionne, M. S. and Harland, R. M. (2003). Gremlin is the BMP antagonist required for maintenance of Shh and Fgf signals during limb patterning. *Nat. Genet.* **34**, 303-307.

Kimmel, R. A., Turnbull, D. H., Blanquet, V., Wurst, W., Loomis, C. A. and Joyner, A. L. (2000). Two lineage boundaries coordinate vertebrate apical ectodermal ridge formation. *Genes Dev.* **14**, 1377-1389.

Lallemand, Y., Nicola, M. A., Ramos, C., Bach, A., Cloment, C. S. and Robert, B. (2005). Analysis of Msx1; Msx2 double mutants reveals multiple roles for Msx genes in limb development. *Development* **132**, 3003-3014.

Lewandoski, M., Sun, X. and Martin, G. R. (2000). Fgf8 signalling from the AER is essential for normal limb development. *Nat. Genet.* **26**, 460-463.

Liu, W., Sun, X., Braut, A., Mishina, Y., Behringer, R. R., Mina, M. and Martin, J. F. (2005). Distinct functions for Bmp signaling in lip and palate fusion in mice. *Development* **132**, 1453-1461.

Loomis, C. A., Kimmel, R. A., Tong, C. X., Michaud, J. and Joyner, A. L. (1998). Analysis of the genetic pathway leading to formation of ectopic apical ectodermal ridges in mouse Engrailed-1 mutant limbs. *Development* **125**, 1137-1148.

Lu, P., Minowada, G. and Martin, G. R. (2006). Increasing Fgf4 expression in the mouse limb bud causes polysyndactyly and rescues the skeletal defects that result from loss of Fgf8 function. *Development* **133**, 33-42.

MacDonald, B. T., Adamska, M. and Meisler, M. H. (2004). Hypomorphic expression of Dkk1 in the doubleridge mouse: dose dependence and compensatory interactions with Lrp6. *Development* **131**, 2543-2552.

Macias, D., Ganan, Y., Ros, M. A. and Hurle, J. M. (1996). In vivo inhibition of programmed cell death by local administration of FGF-2 and FGF-4 in the interdigital areas of the embryonic chick leg bud. *Anat. Embryol.* **193**, 533-541.

Macias, D., Ganan, Y., Sampath, T. K., Piedra, M. E., Ros, M. A. and Hurle, J.

M. (1997). Role of BMP-2 and OP-1 (BMP-7) in programmed cell death and skeletogenesis during chick limb development. *Development* **124**, 1109-1117.
Mahmood, R., Bresnick, J., Hornbruch, A., Mahony, C., Morton, N., Colquhoun, K., Martin, P., Lumsden, A., Dickson, C. and Mason, I. (1995). A role for FGF-8 in the initiation and maintenance of vertebrate limb bud outgrowth. *Curr. Biol.* **5**, 797-806.
Malashichev, Y., Borkhvardt, V., Christ, B. and Scaal, M. (2005). Differential regulation of avian pelvic girdle development by the limb field ectoderm. *Anat. Embryol.* **210**, 187-197.
Martin, G. R. (1998). The roles of FGFs in the early development of vertebrate limbs. *Genes Dev.* **12**, 1571-1586.
Merino, R., Ganan, Y., Macias, D., Rodriguez-Leon, J. and Hurle, J. M. (1999a). Bone morphogenetic proteins regulate interdigital cell death in the avian embryo. *Ann. N. Y. Acad. Sci.* **887**, 120-132.
Merino, R., Rodriguez-Leon, J., Macias, D., Ganan, Y., Economides, A. N. and Hurle, J. M. (1999b). The BMP antagonist Gremlin regulates outgrowth, chondrogenesis and programmed cell death in the developing limb. *Development* **126**, 5515-5522.
Michos, O., Panman, L., Vintersten, K., Beier, K., Zeller, R. and Zuniga, A. (2004). Gremlin-mediated BMP antagonism induces the epithelial-mesenchymal feedback signaling controlling metanephric kidney and limb organogenesis. *Development* **131**, 3401-3410.
Mills, A. A., Zheng, B., Wang, X. J., Vogel, H., Roop, D. R. and Bradley, A. (1999). p63 is a p53 homologue required for limb and epidermal morphogenesis. *Nature* **398**, 708-713.
Min, H., Danilenko, D. M., Scully, S. A., Bolon, B., Ring, B. D., Tarpley, J. E., DeRose, M. and Simonet, W. S. (1998). Fgf-10 is required for both limb and lung development and exhibits striking functional similarity to Drosophila branchless. *Genes Dev.* **12**, 3156-3161.
Mishina, Y., Suzuki, A., Ueno, N. and Behringer, R. R. (1995). Bmpr encodes a type I bone morphogenetic protein receptor that is essential for gastrulation during mouse embryogenesis. *Genes Dev.* **9**, 3027-3037.
Mishina, Y., Hanks, M. C., Miura, S., Tallquist, M. D. and Behringer, R. R. (2002). Generation of Bmpr/Alk3 conditional knockout mice. *Genesis* **32**, 69-72.
Montero, J. A., Ganan, Y., Macias, D., Rodriguez-Leon, J., Sanz-Ezquerro, J. J., Merino, R., Chimal-Monroy, J., Nieto, M. A. and Hurle, J. M. (2001). Role of FGFs in the control of programmed cell death during limb development. *Development* **128**, 2075-2084.
Moon, A. M. and Capecchi, M. R. (2000). Fgf8 is required for outgrowth and patterning of the limbs. *Nat. Genet.* **26**, 455-459.
Moon, A. M., Boulet, A. M. and Capecchi, M. R. (2000). Normal limb development in conditional mutants of Fgf4. *Development* **127**, 989-996.
Mukhopadhyay, M., Shtrom, S., Rodriguez-Esteban, C., Chen, L., Tsukui, T., Gomer, L., Dorward, D. W., Glinka, A., Grinberg, A., Huang, S. P. et al. (2001). Dickkopf1 is required for embryonic head induction and limb morphogenesis in the mouse. *Dev. Cell* **1**, 423-434.
Ngo-Muller, V. and Muneoka, K. (2000). Influence of FGF4 on digit morphogenesis during limb development in the mouse. *Dev. Biol.* **219**, 224-236.
Niswander, L. (2002). Interplay between the molecular signals that control vertebrate limb development. *Int. J. Dev. Biol.* **46**, 877-881.
Niswander, L. and Martin, G. R. (1992). Fgf-4 expression during gastrulation, myogenesis, limb and tooth development in the mouse. *Development* **114**, 755-768.
Niswander, L. and Martin, G. R. (1993). FGF-4 and BMP-2 have opposite effects on limb growth. *Nature* **361**, 68-71.
Niswander, L., Tickle, C., Vogel, A., Booth, I. and Martin, G. R. (1993). FGF-4 replaces the apical ectodermal ridge and directs outgrowth and patterning of the limb. *Cell* **75**, 579-587.
Onichtchouk, D., Chen, Y. G., Dosch, R., Gawantka, V., Delius, H., Massague, J. and Niehrs, C. (1999). Silencing of TGF-beta signalling by the pseudoreceptor BAMBI. *Nature* **401**, 480-485.
Pan, Y., Lin, M. H., Tian, X., Cheng, H. T., Gridley, T., Shen, J. and Kopan, R. (2004). gamma-secretase functions through Notch signaling to maintain skin appendages but is not required for their patterning or initial morphogenesis. *Dev. Cell* **7**, 731-743.
Pan, Y., Liu, Z., Shen, J. and Kopan, R. (2005). Notch1 and 2 cooperate in limb ectoderm to receive an early Jagged2 signal regulating interdigital apoptosis. *Dev. Biol.* **286**, 472-482.
Perantoni, A. O., Timofeeva, O., Naillat, F., Richman, C., Pajni-Underwood, S., Wilson, C., Vainio, S., Dove, L. F. and Lewandoski, M. (2005). Inactivation of FGF8 in early mesoderm reveals an essential role in kidney development. *Development* **132**, 3859-3871.
Pizard, A., Haramis, A., Carrasco, A. E., Franco, P., Lopez, S. and Paganelli, A. (2004). Whole-mount in situ hybridization and detection of RNAs in vertebrate embryos and isolated embryos and isolated organs. In *Current Protocols in Molecular Biology* (ed. F. M. Ausubel, R. Brent, R. E. Kingston, D. D. Moore, J. G. Seidman, J. A. Smith and K. Struhl), pp. 14.9-14.10. New York: Wiley.
Pizette, S. and Niswander, L. (1999). BMPs negatively regulate structure and function of the limb apical ectodermal ridge. *Development* **126**, 883-894.
Pizette, S., Abate-Shen, C. and Niswander, L. (2001). BMP controls proximodistal outgrowth, via induction of the apical ectodermal ridge, and dorsoventral patterning in the vertebrate limb. *Development* **128**, 4463-4474.
Richardson, M. K. and Oelschlager, H. H. (2002). Time, pattern, and heterochrony: a study of hyperphalangy in the dolphin embryo flipper. *Evol. Dev.* **4**, 435-444.
Salas-Vidal, E., Valencia, C. and Covarrubias, L. (2001). Differential tissue growth and patterns of cell death in mouse limb autopod morphogenesis. *Dev. Dyn.* **220**, 295-306.
Sanz-Ezquerro, J. J. and Tickle, C. (2003). Fgf signaling controls the number of phalanges and tip formation in developing digits. *Curr. Biol.* **13**, 1830-1836.
Saunders, J. W. J. (1948). The proximo-distal sequence of the origin of the parts of the chick wing and the role of the ectoderm. *J. Exp. Zool.* **108**, 363-404.
Sekine, K., Ohuchi, H., Fujiwara, M., Yamasaki, M., Yoshizawa, T., Sato, T., Yagishita, N., Matsui, D., Koga, Y., Itoh, N. et al. (1999). Fgf10 is essential for limb and lung formation. *Nat. Genet.* **21**, 138-141.
Sidow, A., Bulotsky, M. S., Kerrebrock, A. W., Bronson, R. T., Daly, M. J., Reeve, M. P., Hawkins, T. L., Birren, B. W., Jaenisch, R. and Lander, E. S. (1997). Serrate2 is disrupted in the mouse limb-development mutant syndactylism. *Nature* **389**, 722-725.
Soriano, P. (1999). Generalized lacZ expression with the ROSA26 Cre reporter strain. *Nat. Genet.* **21**, 70-71.
Soshnikova, N., Zechner, D., Huelsken, J., Mishina, Y., Behringer, R. R., Taketo, M. M., Crenshaw, E. B., 3rd and Birchmeier, W. (2003). Genetic interaction between Wnt/beta-catenin and BMP receptor signaling during formation of the AER and the dorsal-ventral axis in the limb. *Genes Dev.* **17**, 1963-1968.
Storm, E. E., Rubenstein, J. L. and Martin, G. R. (2003). Dosage of Fgf8 determines whether cell survival is positively or negatively regulated in the developing forebrain. *Proc. Natl. Acad. Sci. USA* **100**, 1757-1762.
Summerbell, D. (1974). A quantitative analysis of the effect of excision of the AER from the chick limb-bud. *J. Embryol. Exp. Morphol.* **32**, 651-660.
Sun, X., Lewandoski, M., Meyers, E. N., Liu, Y. H., Maxson, R. E., Jr and Martin, G. R. (2000). Conditional inactivation of Fgf4 reveals complexity of signalling during limb bud development. *Nat. Genet.* **25**, 83-86.
Sun, X., Mariani, F. V. and Martin, G. R. (2002). Functions of FGF signalling from the apical ectodermal ridge in limb development. *Nature* **418**, 501-508.
Thewissen, J. G., Cohn, M. J., Stevens, L. S., Bajpai, S., Heyning, J. and Horton, W. E., Jr (2006). Developmental basis for hind-limb loss in dolphins and origin of the cetacean bodyplan. *Proc. Natl. Acad. Sci. USA* **103**, 8414-8418.
Tickle, C. (2006). Making digit patterns in the vertebrate limb. *Nat. Rev. Mol. Cell Biol.* **7**, 45-53.
Trumpp, A., Depew, M. J., Rubenstein, J. L., Bishop, J. M. and Martin, G. R. (1999). Cre-mediated gene inactivation demonstrates that FGF8 is required for cell survival and patterning of the first branchial arch. *Genes Dev.* **13**, 3136-3148.
Wang, C. K., Omi, M., Ferrari, D., Cheng, H. C., Lizarraga, G., Chin, H. J., Upholt, W. B., Dealy, C. N. and Kosher, R. A. (2004). Function of BMPs in the apical ectoderm of the developing mouse limb. *Dev. Biol.* **269**, 109-122.
Weatherbee, S. D., Behringer, R. R., Rasweiler, J., IV, and Niswander, L. A. (2006). Interdigital webbing retention in bat wings illustrates genetic changes underlying amniote limb diversification. *Proc. Natl. Acad. Sci. USA* **103**, 15103-15107.
Xu, J., Liu, Z. and Ornitz, D. M. (2000). Temporal and spatial gradients of Fgf8 and Fgf17 regulate proliferation and differentiation of midline cerebellar structures. *Development* **127**, 1833-1843.
Yang, A., Schweitzer, R., Sun, D., Kaghad, M., Walker, N., Bronson, R. T., Tabin, C., Sharpe, A., Caput, D., Crum, C. and McKeon, F. (1999). p63 is essential for regenerative proliferation in limb, craniofacial and epithelial development. *Nature* **398**, 714-718.
Yokouchi, Y., Sakiyama, J., Kameda, T., Iba, H., Suzuki, A., Ueno, N. and Kuroiwa, A. (1996). BMP-2/-4 mediate programmed cell death in chicken limb buds. *Development* **122**, 3725-3734.
Yoon, B. S. and Lyons, K. M. (2004). Multiple functions of BMPs in chondrogenesis. *J. Cell. Biochem.* **93**, 93-103.
Zou, H. and Niswander, L. (1996). Requirement for BMP signaling in interdigital apoptosis and scale formation. *Science* **272**, 738-741.
Zucker, R. M., Hunter, E. S., 3rd, and Rogers, J. M. (1999). Apoptosis and morphology in mouse embryos by confocal laser scanning microscopy. *Methods* **18**, 473-480.
Zuniga, A., Haramis, A. P., McMahon, A. P. and Zeller, R. (1999). Signal relay by BMP antagonism controls the SHH/FGF4 feedback loop in vertebrate limb buds. *Nature* **401**, 598-602.
Zuniga, A., Michos, O., Spitz, F., Haramis, A. P., Panman, L., Galli, A., Vintersten, K., Klasen, C., Mansfield, W., Kuc, S. et al. (2004). Mouse limb deformity mutations disrupt a global control region within the large regulatory landscape required for Gremlin expression. *Genes Dev.* **18**, 1553-1564.
Zuzarte-Luis, V. and Hurle, J. M. (2002). Programmed cell death in the developing limb. *Int. J. Dev. Biol.* **46**, 871-876.
Zuzarte-Luis, V. and Hurle, J. M. (2005). Programmed cell death in the embryonic vertebrate limb. *Semin. Cell Dev. Biol.* **16**, 261-269.